Experimental Observation of Batchelor Dispersion of Passive Tracers

Marie-Caroline Jullien,[1] Patrizia Castiglione,[1,2] and Patrick Tabeling[1]

[1]*Laboratoire de Physique Statistique, Ecole Normale Supérieure, 24 rue Lhomond, 75231 Paris, France*

[2]*INFM sezione Roma I, Piazzale Aldo Moro 2, 00185 Roma, Italy*

(Received 1 October 1999; revised manuscript received 2 February 2000)

We report the first detailed experimental observation of the Batchelor regime [G. K. Batchelor, J. Fluid. Mech. **5**, 113 (1959)], in which a passive scalar is dispersed by a large scale strain, at high Péclet numbers. The observation is performed in a controlled two-dimensional flow, forced at large scale, in conditions where a direct enstrophy cascade develops [J. Paret, M.-C. Jullien, and P. Tabeling, Phys. Rev. Lett. **83**, 3418 (1999)]. The expected k^{-1} spectrum is observed, along with exponential tails for the distributions of the concentration and concentration increments and logarithmlike behavior for the structure functions. These observations, confirmed by using simulated particles, provide a support to the theory.

PACS numbers: 47.27.Qb

Turbulent dispersion of passive tracers is involved in a considerable number of situations, pertaining to industrial, geophysical, and astrophysical contexts [1,2]. The problem raises formidable theoretical difficulties, even in the simplest cases where isotropy and homogeneity are assumed to hold. Pathways were opened thirty years ago by Batchelor and Kraichnan [3–5], and recently, owing to the efforts of various groups, substantial progress has been made [6–8].

We now have a "solution" to the problem of turbulent dispersion, in the special case when a dye of low diffusivity is dispersed by a random, time varying, single large scale velocity field for both 2D and 3D [6–8]. Such a situation corresponds to the "Batchelor regime." In the classical view, the Batchelor regime is three dimensional: it corresponds to the case where a tracer is injected on a scale below the Kolmogorov scale, in a turbulent three-dimensional flow. In two dimensions, the Batchelor regime refers to a situation where the tracer is simply dispersed by a smooth 2D, chaotic, velocity field, characterized by a single large scale L [9]. Here solution means that the two-point statistics of the scalar field has been calculated under controlled approximation, which is the achievement of [6–8]. The solution thereby does not rely on a closure scheme. At the present time, conditions under which this theory applies do not seem fully settled, in particular, regarding the energy spectrum. According to [6–8], the theory applies whenever the velocity field is statistically homogeneous, isotropic, and stationary, and its energy spectrum is steeper than k^{-3} at large wave numbers. In such conditions, it is expected the scalar variance spectrum $E_\theta(k)$ decreases as k^{-1}, the second order structure function has a logarithmlike behavior, and the scalar distributions, both for the fluctuations and the increment, develop exponential tails. For the special case where the energy spectrum is in the form $E(k) \sim k^{-3}$, information has been provided [10]: the structure functions have been calculated and a method for determining the form of the probability density functions (PDFs) has been devised. According to this, exponential tails are also expected. The situation does not seem, however, completely settled; recently, issues concerning the energy spectrum exponent required for the theory to apply have been raised [11]. In particular, it has been argued that the energy spectrum should be steeper than k^{-4} for the theory to hold. This point seems potentially controversial.

Turbulent dispersion has received a number of investigations, both experimental and numerical. On the numerical side, one may mention recent direct numerical simulations, which confirmed the relevance of the k^{-1} spectral law in 3D isotropic turbulence [12]. On the experimental side, the situation is somewhat puzzling. Several investigators find the expected k^{-1} spectrum [1,2,13], while others obtain different power laws, or no power law at all [14–16]. To explain such a diversity, one often underlines the possible role of anisotropy, or the importance of coherent structures; it moreover seems legitimate to ask whether theories, based on isotropy and homogeneity assumptions, or hypothesizing self-similarity, are too simplistic to uncover the physical reality. In this context, it seemed to us valuable to investigate whether the predictions of [6–8], based on simplified assumptions, have physical support, and in case sizable deviations are observed, and attempt to characterize them. This is the objective of the present work.

The phenomenon we investigate here is the spreading of a low diffusivity dye in a 2D turbulent flow, forced at large scales. The experimental setup we use has been described previously [17]. The flow is generated in a square PVC cell, 15 cm $\times$ 15 cm. The bottom of the cell is made of a thin (1 mm) glass plate, below which permanent magnets, 5 $\times$ 8 $\times$ 4 mm in size are placed. In order to ensure two dimensionality, the cell is filled with two layers of NaCl solutions, each 3 mm thick, with different densities, $\rho_1 = 1030\ \mathrm{g\,l^{-1}}$ and $\rho_2 = 1060\ \mathrm{g\,l^{-1}}$, placed in a stable configuration, i.e., the heavier underlying the lighter. The interaction of an electrical current driven across the cell with the magnetic field produces local stirring forces. In the experiments we describe here, the experimental conditions of [18] have been reproduced: the magnets are

 0031-9007/00/85(17)/3636(4)$15.00

arranged in four triangular blocks, so as the energy is injected, on average, at a scale of 10 cm; the excitation is permanently maintained. In such conditions, as reported in [18], the flow develops, after a short transient, a direct enstrophy cascade with Kolmogorov-Kraichnan scaling, $E(k) \sim k^{-3}$; the homogeneity and isotropy properties of this regime have been checked. Moreover, the correlation time of the velocity field is finite so that this field follows [6–8] assumptions. The characteristic scale of the motion, L, defined as the maximum of the energy spectrum, is found to be 10 cm.

The passive scalar is a mixture of fluorescein and water, of density $\rho = 1030\ \mathrm{g\,l^{-1}}$, and diffusivity $\kappa = 10^{-6}\ \mathrm{cm^2\,s^{-1}}$. In most cases, the dye matches the upper layer density, and is vertically homogeneously spread across it, throughout the experiment. In several cases we have used a lighter dye, of density $\rho = 1002\ \mathrm{g\,l^{-1}}$ i.e., 3% lighter than the upper layer, so as to operate with thin dye sheets. The concentration field, illuminated by ultraviolet light, is visualized using a 512×512 CCD camera. We have checked that the intensity is proportional to the dye concentration. The images are stored and further processed. The overall spatial resolution for the concentration field is 0.2 mm. The "molecular" Péclet number UL/κ (where U is a typical velocity of the flow—roughly 1 cm/s) is on the order of 10^7. To inject the dye, we first enclose a blob of dye within a cylinder, 5 cm in diameter, in the upper layer, then switch the electrical current on, wait until the transient state vanishes, and eventually delicately remove the cylinder. In these experiments, the flow is statistically stationary, while the concentration field is in a freely decaying regime. Owing to the experimental conditions at hand (large scale forcing for the flow, high Péclet numbers), we may expect the Batchelor regime to take place for the dispersion of the tracer.

Additionally, in order to facilitate the analysis of the experimental observations, we have simulated the concentration field, using a method similar to [19]: the trajectories of 6×10^5 particles, located initially in a disk, 5 cm in diameter, are calculated by integrating the experimentally measured velocity field. Coarsed graining is further applied to generate a concentration field. The simulation is thus designed to mimic the experiment. We will incorporate the results of this work in the discussion of the physical experimental results.

Figure 1 shows a typical evolution of a spot of fluorescein 5 cm in diameter, released in the system at time $t = 0$. At an early time, the blob is localized in the center of the cell, and is slightly distorted. It is further vigorously advected, strained, and folded. At this stage, the striations display a broad range of sizes, as displayed in Fig. 1. After a period of 30 s the concentration field is homogeneous; we have checked, by sampling the fluid, that the dye remains confined in the upper layer, throughout the mixing process. In this system, mixing seems homogeneous and there is no evidence of the presence of any long-lived structure

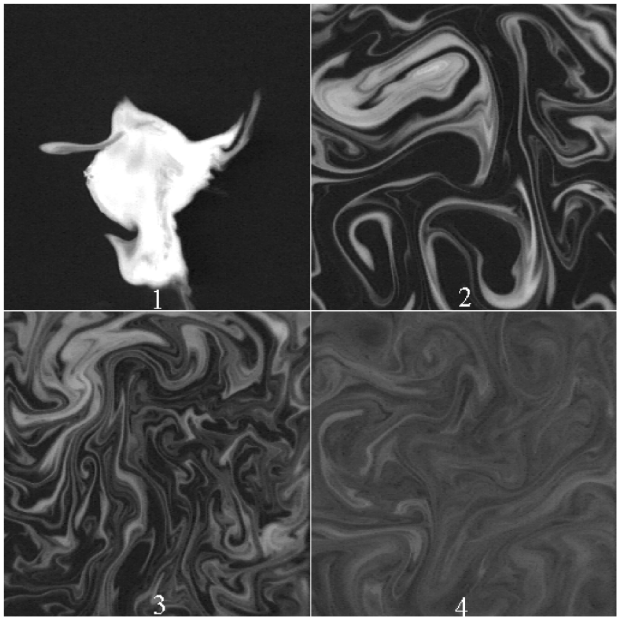

FIG. 1. Time evolution of a blob of fluoresceine of density $\rho = 1002\ \mathrm{g\,l^{-1}}$ in a 16 cm $\times$ 16 cm region, at times $t = 1$, 12, 20, and 40 s.

trapping the tracer throughout the duration of the experiment. We believe this is due to the particular forcing we use, which disrupts the coherent structures, a requirement for the development of an enstrophy cascade [18], and probably also for that of a Batchelor regime.

Figure 2 shows the evolution of the dissipation spectrum $k^2 E_\theta(k)$ [where k is the wave number and $E_\theta(k)$ is the variance spectrum of the concentration field], corresponding to the sequence of Fig. 1. Each dissipation spectrum is averaged over 1 s then slightly smoothed. At early times, the dissipation is dominated by a bump, localized at a wave number corresponding to the initial drop size. Between $t = 8$ and 18 s, the spectra show the same characteristics:

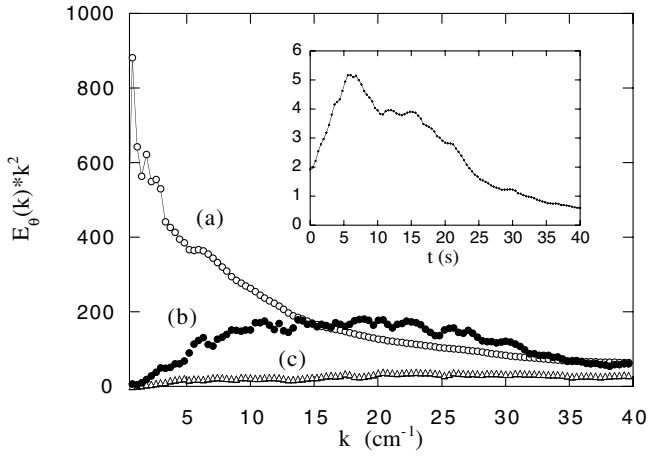

FIG. 2. Evolution of the dissipation spectrum of a $\rho = 1002\ \mathrm{g\,l^{-1}}$ density pollutant, at times (a) $t = 1$, (b) $t = 12$, and (c) $t = 40$ s. Inset shows the total dissipation versus time.

they gradually increase up to $k = 12\ \mathrm{cm}^{-1}$, then decrease. At later times, the dissipation spectrum progressively collapses; it keeps evolving with time up to a final stage where equipartition is obtained, corresponding to complete mixing. The existence of a range of time, comprised between 8 and 18 s, where the concentration field seems to reach a quasistationary state is confirmed by the inspection of the total dissipation, $\int k^2 E(k)$ (inset in Fig. 2), which displays a broad maximum in this range of time. In such a range, we are in a framework consistent with the assumptions made in the theory, concerning statistical stationarity [8]. We further concentrate on the analysis of this region, which we call the "quasistationary domain."

Figure 3 displays the scalar variance spectrum, now averaged over the entire quasistationary domain, along with the compensated spectrum $kE_\theta(k)$. The scalar variance spectrum $E_\theta(k)$ is expected to evolve as $E_\theta(k) \approx -\chi/\gamma k$, where γ is a mean rate of strain, and $\chi = 2\kappa\langle(\nabla\theta)^2\rangle$ is the scalar dissipation. The spectrum displays a range of wave numbers, between 1 and 7 cm^{-1}, where a k^{-1} law fairly holds. As expected, the range of scales in which the power law is observed is well above the characteristic wave number of the motion, estimated to 0.7 cm^{-1}. Beyond $k = 7\ \mathrm{cm}^{-1}$, the spectrum drops. This defines an effective dissipation wave number for our experiment. This quantity is well below the Batchelor wave number $k_B = (\gamma/\kappa)^{1/2}$, which in our case should be on the order of 2800 cm^{-1}. The dissipation scale of the experiment originates in the fact that at each inversion of the electrical current, a transient shear develops in the upper layer, enhancing tracer diffusion in the horizontal plane. This cutoff can be substantially shifted (by a factor of 2, roughly), by working with tracer sheets of different thicknesses. The numerical simulation we performed, in which such a phenomenon is irrelevant, led to the same spectrum as in the experiment, indicating our results are probably not contaminated by this effect, in the inertial convective range.

We now turn to the measurement of the PDFs of scalar fluctuations $P[\theta(\mathbf{x}) - \langle\theta(\mathbf{x})\rangle]$, a crucial quantity to consider for comparing with theory. Figure 4 displays the PDFs at $t = 8$ s and $t = 16$ s, i.e., well within the quasistationary interval. The PDF is representative of the distributions observed throughout the interval. They are strikingly different from those observed at earlier times (which are bimodal) and at later times (which are Gaussian). The PDFs of the quasistationary domain are nonsymmetric and non-Gaussian: as shown in Fig. 4, they develop exponential tails, on the positive side and Gaussian behavior, on the negative one. The tails seem controlled by the fronts, located at the edges of the tracer filaments. Here again, the numerical simulation shows the same results. These characteristics of the PDFs of the concentration field are in good qualitative agreement with the theoretical analysis in [6–8].

Another quantity of interest is the standardized (i.e., rescaled so as the variance be unity) PDFs of the concentration increments defined by

$$\Delta\theta = \theta(\mathbf{x} + \mathbf{r}) - \theta(\mathbf{x}),$$

where r is the scale. Figure 5 displays such PDFs, at time $t = 16$ s in the quasistationary domain for various scales. These PDFs appear self-similar in space, and roughly symmetric. The small increment region looks Gaussian while the tails, defined for increments above 1 standard deviation, may be fitted by exponential functions. We thus have here a Gaussian bump with exponential tails. These findings agree well with the theory since for k^{-3} or steeper spectra, one expects exponential tails. In the inset, we show the corresponding distributions obtained by using a simulated concentration field; they are similar to the experiment.

As is traditionally done for turbulent signals, we measure the structure functions of the concentration increments defined by

$$S_p = \langle[\theta(\mathbf{x} + \mathbf{r}) - \theta(\mathbf{x})]^p\rangle.$$

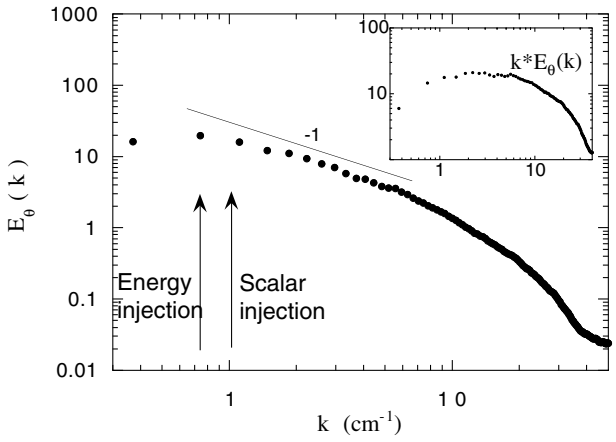

FIG. 3. Variance scalar spectra with a pollutant of density $\rho = 1002\ \mathrm{g\,l}^{-1}$; the straight line has a k^{-1} slope. The inset shows the compensated spectra $E_\theta(k) \times k$.

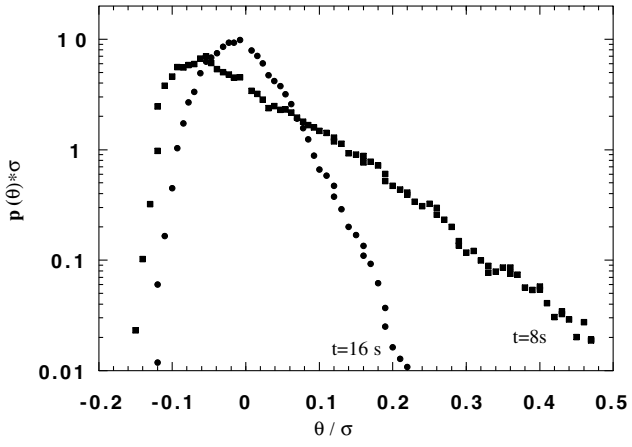

FIG. 4. Rescaled distributions of the fluctuations of concentration at times $t = 8$ s and $t = 16$ s. The passive scalar used has density $\rho = 1002\ \mathrm{g\,l}^{-1}$.

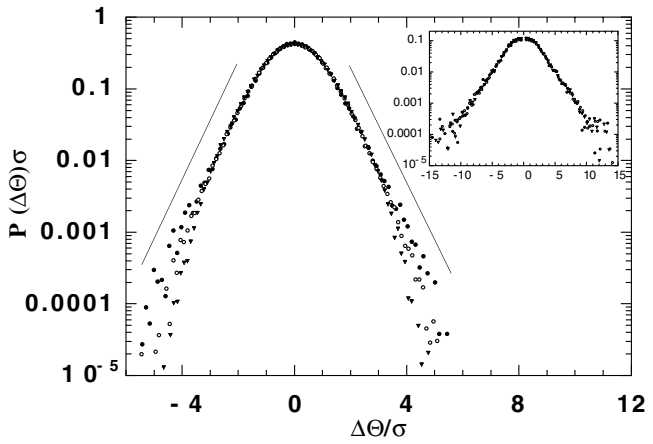

FIG. 5. Rescaled distributions of the concentration increments at time $t = 16$ s for three different increments in the Batchelor range for a $\rho = 1002\ \mathrm{g\,l^{-1}}$ density pollutant. Full squares correspond to $r = 1.165$ cm, empty squares to $r = 4.078$ cm, and triangles down to $r = 6.991$ cm. The inset shows the numerical result for the same increments at the same time.

Figure 6 displays such structure functions as a function of the scale r, up to order eighth. The scaling range corresponding to the inertial convective domain is difficult to determine accurately; it roughly lies between $r = 0.3$ and 5 cm. In this range, there is no clear power law, and one may propose logarithmic laws for representing these functions. In the framework of the Chertkov *et al.* [6] theory the fit formula we propose for $S_2(r)$ corresponds to the case where, in the enstrophy cascade, the logarithmic corrections are small (which appears to be the case in our experiment [18]). We thus have consistency between the theory and the experiment. It is certainly difficult to say much more at the moment.

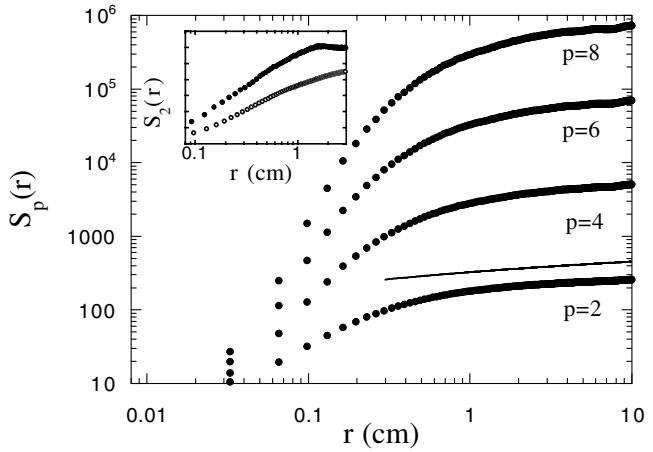

FIG. 6. Even structure functions up to the order of 8. Straight line is a logarithmic fit for $S_2(r)$, $S_2(r) \approx 300 + 55\ln(r/L)$. The passive scalar used has the density $\rho = 1002\ \mathrm{g\,l^{-1}}$. The numerical result for $S_2(r)$ (full circles) is shown in the inset with linear-log axis, compared to the experimental ones (empty circles).

To summarize, we have investigated the Batchelor regime, for a free decaying blob of a passive scalar, in a physical experiment. We have observed k^{-1} spectrum, exponential tails for the distributions of the concentration and concentration increments, and logarithmic behavior for the second order structure functions. These findings have been confirmed by using simulated particles. Compared to [15], we have concentrated on larger scales to dig out the Batchelor regime and this is probably why we reach different conclusions. Our observations turn out to be extremely consistent with the theoretical analysis of [6–8]. Perhaps more work is needed to settle the validity range of the theory. Nonetheless, the statement we can make at the moment is that the experimental study provides substantial support to a theoretical analysis which has successfully calculated the two-point statistics of the field, without calling for a closure scheme, a situation particularly rare in the field.

This work was supported by the CNRS, the ENS, the Universités Paris 6 and Paris 7, and Contract No. ERBFMRXCT980175 "Intermittency in turbulent systems." We acknowledge valuable discussions with A. Babiano, G. Falkovich, A. Fouxon, K. Gawedsky, B. Shraiman, and M. Vergassola.

[1] H. L. Grant, B. A. Hugues, R. B. Williams, and A. Moillet, J. Fluid Mech. **34**, 423 (1968).
[2] N. S. Oakey, J. Phys. Oceanogr. **12**, 256 (1982).
[3] G. K. Batchelor, J. Fluid Mech. **5**, 113 (1959).
[4] R. Kraichnan, Phys. Fluids **10**, 1417 (1967).
[5] R. Kraichnan, Phys. Fluids **11**, 945 (1968).
[6] M. Chertkov, G. Falkovich, I. Kolokolov, and V. Lebedev, Phys. Rev. E **51**, 5609 (1995).
[7] G. Falkovich, I. Kolokolov, V. Lebedev and A. Migdal, Phys. Rev. E **54**, 4896 (1996).
[8] E. Balkovsky and A. Fouxon, Phys. Rev. E **60**, 4164 (1999).
[9] A. Crisanti, M. Falcioni, G. Paladin, and A. Vulpiani, Physica (Amsterdam) **166A**, 305 (1990).
[10] G. Falkovich (private communication).
[11] M. A. Khan and J. C. Vassilicos (to be published).
[12] D. Bogucki, J. A. Domaradzki, and P. K. Yeung, J. Fluid Mech. **343**, 111 (1997).
[13] C. H. Gibson and W. H. Scharz, J. Fluid Mech. **16**, 365 (1963).
[14] A. Gargett, J. Fluid Mech. **159**, 379 (1985).
[15] B. S. Williams, D. Marteau, and J. P. Gollub, Phys. Fluids **9**, 2061 (1997).
[16] P. L. Miller and P. E. Dimotakis, J. Fluid Mech. **308**, 129 (1996).
[17] J. Paret and P. Tabeling, Phys. Fluids **10**, 3126 (1998).
[18] J. Paret, M.-C. Jullien, and P. Tabeling, Phys. Rev. Lett. **83**, 3418 (1999).
[19] M.-C. Jullien, J. Paret, and P. Tabeling, Phys. Rev. Lett. **82**, 2872 (1999).